

## Supplemental Figure Legends

**Supplemental Figure 1. Activation of the IRE-1/XBP-1 pathway in B cells.** Activation of IRE-1 begins in the lumen of the ER via oligomerization, which allows autophosphorylation to occur to regulate IRE-1's RNase activity in the cytoplasm. In human and mouse B cells, active IRE-1 RNase subsequently splices 26 nucleotides from the XBP-1 mRNA, causing a translational frame-shift. The spliced mRNA encodes a 54-kDa XBP-1 transcription factor that translocates into the nucleus to regulate the expression of genes that are important for B-cell functions.

**Supplemental Figure 2. B or CLL cell purification from spleens of XBP-1<sup>WT</sup>/E $\mu$ -TCL1 and XBP-1<sup>KO</sup>/E $\mu$ -TCL1 mice.** (A) Splenocytes (left panel) from 6-week-old XBP-1<sup>WT</sup>/E $\mu$ -TCL1 mice were purified using Pan B Cell Isolation MicroBeads (middle panel) and stained with CD3-APC-Cy7, IgM-PE-Cy7, B220-FITC and CD5-APC monoclonal antibodies. CD3+/IgM- T cells and the majority of CD3-/IgM-non-B/non-T cells were removed successfully. Gated CD3-/IgM+ B cells were analyzed for the expression of B220 and CD5 (right panel). Data are representative of three independent experiments. (B-C) Splenocytes (left panel) from 14-month-old XBP-1<sup>WT</sup>/E $\mu$ -TCL1 (B) and XBP-1<sup>KO</sup>/E $\mu$ -TCL1 (C) mice were purified using Pan B Cell MicroBeads (middle panel), and stained with monoclonal antibodies as described in (A), Gated CD3-/IgM+ B cell populations were analyzed for the expression of B220 and CD5 (right panel). Data are representative of three independent experiments.

**Supplemental Figure 3. Genetic XBP-1 deficiency does not affect synthesis, assembly and intracellular transport of class I and class II MHC molecules.** (A-B) CLL cells isolated 12-month-old XBP-1<sup>WT</sup>/E $\mu$ -TCL1 and XBP-1<sup>KO</sup>/E $\mu$ -TCL1 mice were labeled with [<sup>35</sup>S]-methionine and [<sup>35</sup>S]-cysteine for 15 min, chased for the indicated times, and lysed. Lysates were immunoprecipitated using antibodies against the class I MHC (A) or class II MHC (B) molecules. Immunoprecipitates were

analyzed by SDS-PAGE. HC denotes the class I MHC heavy chain; CHO, high mannose-type glycans; and CHO\*, complex-type glycans.

**Supplemental Figure 4. XBP-1 deficiency does not alter certain B cell-critical surface markers in leukemia.** Splenocytes isolated from approximately 9-month-old XBP-1<sup>WT</sup>/E $\mu$ -TCL1 and XBP-1<sup>KO</sup>/E $\mu$ -TCL1 mice were stained with monoclonal antibodies against CD3, IgM, CD5 together with one of the following B cell surface markers: CD1d (**A**), CD49b (**B**), CD20 (**C**), CD24 (**D**), CD38 (**E**), CD184 (**F**), class II MHC (**G**), CD25 (**H**), GL7 (**I**) and CD138 (**J**). The expression of each specific marker on the surface of CD5<sup>-</sup> B cells and CD5<sup>+</sup> CLL cells were analyzed on gated CD3-/IgM<sup>+</sup> B cell populations in the mouse spleens. Data are representative of three independent experiments.

**Supplemental Figure 5. Chemical stability of B-I09.** (**A**) The degradation of B-I09 is plotted as a function of time upon exposure to FRET-suppression assay buffer at room temperature (blue) or cell culture media 37 °C (red). Aliquots were injected onto LCMS (UV monitored at 320 nm) and the peaks integrated. The 1,3-dioxane protecting group in B-I09 is stable to the FRET-suppression assay buffer at room temperature, whereas it exhibits a  $t_{1/2}$  of approximately 30 h in cell culture media (37 °C). (**B**) Representative HPLC trace at  $t = 24$  h for B-I09 in cell culture media, showing the partial degradation of B-I09 and formation of the corresponding aldehyde in the decomposed product, C-B06. (**C**) The dose-response curve of C-B06 in inhibiting human IRE-1 RNase from cleaving mini-XBP-1 stem-loop RNA. Dose-response FRET-suppression experiments were carried out a minimum of 3 times on different days, and IC<sub>50</sub> values were calculated from the mean inhibition value at each concentration. (**D**) MEC1 and MEC2 human CLL cells were treated with DMSO (control) or C-B06 (20  $\mu$ M) for 48 h. Cells were lysed and RNA was extracted for RT-PCR. The expression of human unspliced XBP-1 (XBP-1u), spliced XBP-1 (XBP-1s) and actin was detected using specific primers. Results are representative of three independent experiments. (**E**) Human MEC1 and MEC2 CLL cells were cultured for 48 h in the

presence of DMSO (control) or CB-06 (20  $\mu$ M). Cells were lysed for analysis of the expression of XBP-1s, p97 and actin by immunoblots using specific antibodies. Data shown in immunoblots are representative of three independent experiments.

**Supplemental Figure 6. B-109 specifically affects the synthesis of secretory IgM, but not the synthesis, assembly and transport of membrane-bound IgM, class I MHC molecules and Ig $\alpha$ /Ig $\beta$  heterodimers.** (A-B) Wild-type B cells were stimulated with LPS for 2 days and subsequently treated with DMSO (control) or B-109 (20  $\mu$ M) for additional 1 day. DMSO- or B-109-treated wild-type B cells were radiolabeled for 15 min, chased for indicated times and lysed. Intracellular membrane-bound  $\mu$  chain ( $\mu$ M), secretory  $\mu$  chain ( $\mu$ M) and  $\kappa$  light chain was immunoprecipitated from lysates using an anti- $\kappa$  antibody (A). Secreted  $\mu$  and  $\kappa$  chains were also immunoprecipitated from culture media using an anti- $\kappa$  antibody (B). Immunoprecipitates were analyzed by SDS-PAGE. Data are representative of three independent experiments. (C) Similar lysates as those in (A) were immunoprecipitated using an antibody against the class I MHC heavy chain (HC), and immunoprecipitates were analyzed by SDS-PAGE. CHO and CHO\* denote high mannose-type glycans and complex-type glycans, respectively. Data are representative of three independent experiments. (D) From similar lysates as those in (A), Ig $\alpha$ /Ig $\beta$  heterodimers were immunoprecipitated using an anti-Ig $\beta$  antibody. Immunoprecipitated Ig $\alpha$ /Ig $\beta$  heterodimers were eluted from the beads and treated with endo-H or PNGase F before analyzed by SDS-PAGE. CHO, CHO\*, NAG indicate high mannose-type glycans, complex-type glycan and N-acetylglucosamines, respectively. Data are representative of three independent experiments.

**Supplemental Figure 7. B-109 treatment leads to the upregulated expression of IRE-1.** E $\mu$ -TCL1 B cells were cultured in LPS for 2 days, subsequently treated with B-109 (20  $\mu$ M) for an additional day, and lysed for analysis of the expression of XBP-1s, IRE-1, p97 and actin by immunoblots. Data are representative of two experiments.

**Supplemental Figure 8. CLL cells consist of the majority of lymphocytes in PBMCs from CLL-bearing E $\mu$ -TCL1 mice.** PBMCs from CLL-bearing E $\mu$ -TCL1 mice were stained with CD3-APC-Cy7, IgM-PE-Cy7, B220-FITC and CD5-APC monoclonal antibodies. Gated lymphocyte populations in PBMCs (left panel) were analyzed for CD3+/IgM- T cells, CD3-/IgM- non-B/non-T cells, and CD3-/IgM+ B cells (middle panel). Gated CD3-/IgM+ B cells were analyzed for the expression of B220 and CD5 (right panel). Data are representative of three independent experiments.

**Supplemental Figure 9. B-I09 inhibits the splicing of XBP1 mRNA and synergizes with ibrutinib to suppress the growth of mouse and human multiple myeloma (MM) cell lines.** (A) Mouse 5TGM1 MM cells and human RPMI-8226 MM cells were treated with DMSO (control) or B-I09 (20  $\mu$ M) for 48 h. Cells were lysed to extract RNA for RT-PCR. The expression of mouse and human unspliced XBP-1 (XBP-1u), spliced XBP-1 (XBP-1s) and actin was detected using specific primers. XBP-1 splicing was inhibited by B-I09 in both mouse and human MM cells. (B-E) Dose-dependent growth inhibition curves of mouse 5TGM1 (B), human U266 (C), human RPMI-8226 (D) and human NCI-H929 (E) MM cell lines treated for 48 h with B-I09, ibrutinib, or the combination were determined by CellTiter Blue assays. The concentration ranges for B-I09 and ibrutinib are 3.9  $\mu$ M ~ 100  $\mu$ M and 1.56  $\mu$ M ~ 40  $\mu$ M, respectively. Data derived from 2 identical experimental repeats were plotted as mean  $\pm$  SEM.

**Supplemental Figure 10. B-I09 inhibits the splicing of XBP-1 mRNA and synergizes with ibrutinib to suppress the growth of human mantle cell lymphoma (MCL) cell lines.** (A) Human HBL2, Jeko, Mino and Z138 MCL cell lines were treated with DMSO (control) or B-I09 (20  $\mu$ M) for 48 h. Cells were lysed and RNA was extracted for RT-PCR. The expression of human unspliced XBP-1 (XBP-1u), spliced XBP-1 (XBP-1s) and actin was detected using specific primers. XBP-1 splicing was inhibited by B-I09 in all 4 human MCL cell lines. (B-E) Dose-dependent growth inhibition curves of human HBL2

(B), Jeko (C), Mino (D) and Z138 (E) MCL cell lines treated for 48 h with B-I09, ibrutinib, or the combination were determined by CellTiter Blue assays. The concentration ranges for B-I09 and ibrutinib are 3.9  $\mu$ M ~ 100  $\mu$ M and 1.56  $\mu$ M ~ 40  $\mu$ M, respectively. Data derived from 2 (for HBL2, Jeko and Mino) or 3 (for Z138) identical experimental repeats were plotted as mean  $\pm$  SEM.

**Supplemental Figure 11. B-I09 synergizes with ibrutinib to induce apoptosis in multiple myeloma and mantle cell lymphoma cells.** (A-B) Mouse 5TGM1 MM cells (A) and human Mino MCL cells (B) were cultured in the presence of DMSO (control), B-I09 (20  $\mu$ M), ibrutinib (10  $\mu$ M), or the combination for 48 h (5TGM1) or 72 h (Mino). Cells were lysed for analysis of the expression of XBP-1s, cleaved caspase-3, cleaved PARP, p97 and actin by immunoblots using specific antibodies. Data shown in immunoblots are representative of three independent experiments.

Line	Cancer type	CI at effect levels			CI		rank	n
		0.75	0.9	0.95	mean	SEM		
<b>MEC1</b>	B-Chronic Lymphocytic Leukemia	0.561	0.660	0.761	0.661	0.582	+++	2
<b>MEC2</b>	B-Chronic Lymphocytic Leukemia	0.333	0.276	0.247	0.285	0.139	++++	2
<b>WaC3</b>	B-Chronic Lymphocytic Leukemia	0.335	0.246	0.202	0.261	0.016	++++	2
<b>U266</b>	Multiple Myeloma	0.802	0.780	0.797	0.793	0.249	++	2
<b>RPMI-8226</b>	Multiple Myeloma	0.803	0.655	0.575	0.677	0.119	+++	2
<b>NCI-H929</b>	Multiple Myeloma	0.508	0.425	0.378	0.437	0.163	+++	2
<b>HBL2</b>	Mantle Cell Lymphoma	0.658	0.568	0.518	0.581	0.038	+++	2
<b>Jeko</b>	Mantle Cell Lymphoma	0.941	0.874	0.842	0.886	0.092	+	2
<b>Mino</b>	Mantle Cell Lymphoma	0.906	0.797	0.734	0.813	0.145	++	2
<b>Z138</b>	Mantle Cell Lymphoma	0.849	0.719	0.649	0.739	0.090	++	3

**Supplemental Table 1. Synergism of B-I09 and ibrutinib.** The indicated human cell lines were plated in 384-well plates and then treated concurrently with B-I09 and ibrutinib for 48 h. Cell viability was measured by a CellTiter-Blue assay (Promega), and results were used to calculate the Chou and Talalay combination index (CI) value at effect levels of 0.75, 0.9 and 0.95 as well as the mean value for all three effect levels. CI values represent the mean +/- the standard error of the mean (SEM) for 2 or 3 independent replicate experiments. CI values can be characterized for additivity, synergy or antagonism as described by Chou (Ref. 39). A combination index of <0.3 is represented as ++++ ranking and indicates strong synergism by this method. Other CI symbols and descriptions of combination effects are as follows: 0.3-0.7, +++, synergism; 0.7-0.85, ++, moderate synergism; 0.85 - 0.90, +, slight synergism; 0.90-1.10, and ±, nearly additive.

## Supplementary Information

### *Chemical synthesis general notes*

Unless stated otherwise, reactions were performed in flame-dried glassware under a positive pressure of argon or nitrogen gas using dry solvents. Commercial grade reagents and solvents were used without further purification except where noted. Diethyl ether, toluene, dimethylformamide, dichloromethane, and tetrahydrofuran were purified by a Glass Contour column-based solvent purification system. Other anhydrous solvents were purchased directly from chemical suppliers. Thin-layer chromatography (TLC) was performed using silica gel 60 F254 pre-coated plates (0.25 mm). Flash chromatography was performed using silica gel (60  $\mu\text{m}$  particle size). The purity of all compounds was judged by TLC analysis (single spot/two solvent systems) using a UV lamp, CAM (ceric ammonium molybdate), ninhydrin, or basic  $\text{KMnO}_4$  stain(s) for detection purposes. NMR spectra were recorded on a 400 MHz spectrometer.  $^1\text{H}$  and  $^{13}\text{C}$  NMR chemical shifts are reported as  $\delta$  using residual solvent as an internal standard. Analytical (4 x 150 mm column, 1 mL/min flow rate) RP-HPLC was performed on a  $\text{C}_{18}$  column with acetonitrile/water (0.1% formic acid) as eluent. In the end of Supplementary Information, we have included NMR and HPLC data for the three most important compounds described in this manuscript, B-H09, B-I08 and B-I09. The data show >95% purity in each compound tested. All other compounds used in our studies are also of high purity (>95%).

### *Synthesis of B-B07 (methyl 3-(5-formyl-6-hydroxynaphthalen-2-yl)benzoate)*

A mixture of 6-bromo-2-hydroxy-1-naphthaldehyde (50 mg, 200  $\mu\text{mol}$ ), (3-methoxycarbonyl)phenylboronic acid (45 mg, 250  $\mu\text{mol}$ ), and sodium carbonate (84 mg, 804  $\mu\text{mol}$ ) in 2 mL of 1:1 DMF: $\text{H}_2\text{O}$  was treated with tetrakis(triphenylphosphine)palladium(0) (12 mg, 10  $\mu\text{mol}$ ) and stirred at 100  $^\circ\text{C}$  for 30 min. The reaction was cooled to room temperature, diluted with sat. aq.  $\text{NH}_4\text{Cl}$ , and extracted with  $\text{CHCl}_3$ . The organic layers were dried over  $\text{Na}_2\text{SO}_4$ , concentrated, and the crude residue purified by flash chromatography over silica gel (40% EtOAc/hexanes eluent) to give B-B07 as

a pale yellow solid (12 mg, 19%).  $^1\text{H}$  NMR (400 MHz,  $\text{CDCl}_3$ )  $\delta$  13.17 (s, 1H), 10.85 (s, 1H), 8.44 (d,  $J$  = 8.8 Hz, 1H), 8.38 (t,  $J$  = 1.6 Hz, 1H), 8.07 (s, 1H), 8.05 (d,  $J$  = 4.6 Hz, 2H), 7.93 – 7.87 (m, 2H), 7.57 (t,  $J$  = 8.0 Hz, 1H), 7.20 (d,  $J$  = 9.1 Hz, 1H), 3.98 (s, 3H);  $^{13}\text{C}$  NMR (101 MHz,  $\text{CDCl}_3$ )  $\delta$  193.4, 167.1, 165.2, 140.5, 139.5, 136.3, 132.4, 131.6, 131.0, 129.3, 128.8, 128.5, 128.3, 128.3, 127.6, 120.0, 119.6, 111.4, 52.5; HRMS (ESI-TOF) ( $m/z$ )  $[\text{M}+\text{H}]^+$  calcd for  $\text{C}_{19}\text{HO}_4$  307.09703, found 307.09696.

*Synthesis of B-H10 (allyl (2-(8-formyl-7-hydroxy-2-oxo-2H-chromen-4-yl)ethyl)carbamate)*

A solution of  $\beta$ -alanine (3.00 g, 33.7 mmol) in 50 mL of dioxane: $\text{H}_2\text{O}$  (1:1) was treated with  $\text{Na}_2\text{CO}_3$  (7.15 g, 33.7 mmol) and allyloxychloroformate (3.58 mL, 67.4 mmol). The reaction was stirred for 2 days at room temperature, quenched with 1M aq.  $\text{KHSO}_4$ , and extracted with EtOAc. The combined organic layers were dried over  $\text{Na}_2\text{SO}_4$  and evaporated to afford (*N*-Alloc)- $\beta$ -alanine as a white solid (4.70 g, 97%).

A solution of (*N*-Alloc)- $\beta$ -alanine (4.13 g, 23.87 mmol) in 100 mL of DCM at 0  $^\circ\text{C}$  was treated with 2,2-Dimethyl-1,3-dioxane-4,6-dione (4.47 g, 31.03 mmol), 4-dimethylaminopyridine (2.92 g, 23.9 mmol), and diisopropylcarbodiimide (3.70 mL, 23.9 mmol). The reaction was stirred from 0  $^\circ\text{C}$  to room temperature over 4 h, then washed with 10% aq.  $\text{KHSO}_4$  followed by brine. The organic layer was dried over  $\text{Na}_2\text{SO}_4$  and concentrated. The resulting colorless liquid was dissolved in a 10:1 methanol:toluene mixture and stirred at reflux for 15 h. After cooling, the reaction was concentrated under reduced pressure. Purification by flash column chromatography over silica gel (25%-60% EtOAc/hexanes eluent) afforded methyl 5-(((allyloxy)carbonyl)amino)-3-oxopentanoate as a colorless oil (5.02 g, 91%).  $^1\text{H}$  NMR (400 MHz,  $\text{CDCl}_3$ )  $\delta$  5.97 – 5.82 (m, 1H), 5.37 – 5.12 (m, 3H), 4.53 (d,  $J$  = 5.6 Hz, 2H), 3.73 (s, 3H), 3.50 – 3.37 (m, 4H), 2.80 (t,  $J$  = 5.7 Hz, 2H);  $^{13}\text{C}$  NMR (101 MHz,  $\text{CDCl}_3$ )  $\delta$  202.2, 167.3, 156.2, 132.8, 132.8, 117.6, 117.5, 65.4, 52.4, 52.4, 48.9, 42.8, 35.3; HRMS (ESI-TOF) ( $m/z$ )  $[\text{M}+\text{H}]^+$  calcd for  $\text{C}_{10}\text{H}_{16}\text{NO}_5$  230.10285, found 230.10297.

A solution of 5-(((allyloxy)carbonyl)amino)-3-oxopentanoate (2.31 g, 10.06 mmol) in 50 mL of methanesulfonic acid at 0 °C was treated with resorcinol (1.11 g, 10.06 mmol) and stirred for 3.5 h. The mixture was poured into ice cold water and the resulting yellow mixture was filtered. The filtrate was extracted with EtOAc and combined with the solids. The combined organic layer was concentrated and purified by flash chromatography over silica gel (0-20% MeOH/CHCl<sub>3</sub> eluent) to afford allyl (2-(7-hydroxy-2-oxo-2*H*-chromen-4-yl)ethyl)carbamate as a yellow solid (2.56 g, 88%).<sup>1</sup>H NMR (400 MHz, DMSO-*d*<sub>6</sub>) δ 10.55 (s, 1H), 7.68 (d, *J* = 8.8 Hz, 1H), 7.40 (m, 1H), 6.80 (dd, *J* = 8.7, 2.3 Hz, 1H), 6.71 (d, *J* = 2.3 Hz, 1H), 6.07 (s, 1H), 5.99 – 5.78 (m, 1H), 5.24 (m, 1H), 5.15 (m, 1H), 4.45 (m, 2H), 3.29 (m, 2H), 2.87 (t, *J* = 6.7 Hz, 2H); <sup>13</sup>C NMR (101 MHz, DMSO-*d*<sub>6</sub>) δ 161.1, 160.3, 156.0, 155.2, 154.2, 133.8, 133.7, 126.3, 116.9, 113.0, 111.3, 110.5, 110.4, 102.5, 102.4, 64.3, 31.5, 23.4; HRMS (ESI-TOF) (*m/z*) [M+H]<sup>+</sup> calcd for C<sub>16</sub>H<sub>16</sub>NO<sub>5</sub> 302.10285, found 302.10305.

A solution of allyl (2-(7-hydroxy-2-oxo-2*H*-chromen-4-yl)ethyl)carbamate (0.37 g, 1.28 mmol) in 15 mL of glacial acetic acid was treated with hexamethylenetetramine (0.27 g, 1.92 mmol) and stirred at room temperature for 5.5 h. The reaction mixture was concentrated and the resulting slurry was dissolved in a 1:1 mixture of 1M aq. HCl and EtOAc and stirred at 60 °C for 45 min. The organic layer was separated and the aqueous layer was extracted with EtOAc. The organic layers were concentrated and purified by flash column chromatography over silica gel (35%-100% EtOAc/hexanes eluent) to give B-H10 (allyl (2-(8-formyl-7-hydroxy-2-oxo-2*H*-chromen-4-yl)ethyl)carbamate) as a colorless oil (32 mg, 10%).<sup>1</sup>H NMR (400 MHz, CDCl<sub>3</sub>) δ 12.24 (s, 1H), 10.60 (s, 1H), 7.92 (d, *J* = 9.1 Hz, 1H), 6.93 (d, *J* = 9.0 Hz, 1H), 6.19 (s, 1H), 5.90 (m, 1H), 5.39 – 5.15 (m, 2H), 5.03 (bs, 1H), 4.58 (m, 2H), 3.49 (m, 2H), 2.99 (t, *J* = 7.2 Hz, 2H); <sup>13</sup>C NMR (101 MHz, CDCl<sub>3</sub>) δ 193.5, 193.4, 165.5, 159.2, 156.6, 156.5, 153.4, 133.1, 132.6, 118.2, 114.8, 112.2, 112.1, ,111.1, 109.0, 66.0, 40.1, 32.8; HRMS (ESI-TOF) (*m/z*) [M+H]<sup>+</sup> calcd for C<sub>16</sub>H<sub>16</sub>NO<sub>6</sub> 318.09777, found 318.09746.

*Synthesis of B-H09 (allyl 7-formyl-8-hydroxy-5-oxo-4,5-dihydro-1H-chromeno[3,4-c]pyridine-3(2H)-carboxylate)*

A solution of the allyl (2-(7-hydroxy-2-oxo-2H-chromen-4-yl)ethyl)carbamate intermediate above (0.50 g, 1.73 mmol) in 50 mL of acetonitrile at room temperature was treated with pyridine (0.07 mL, 0.86 mmol) and acetic anhydride (0.82 mL, 8.64 mmol). After stirring for 6 h, the reaction mixture was concentrated and partitioned between EtOAc and brine. The organic layer was dried over Na<sub>2</sub>SO<sub>4</sub> and concentrated. The resulting residue was dissolved in 4 mL of trifluoroacetic acid, treated with hexamethylenetetramine (0.61 g, 4.32 mmol), and refluxed for 20 h. The reaction mixture was concentrated under reduced pressure and the resulting mixture was dissolved in a 1:1 mixture of EtOAc and 1M aq. HCl and stirred at 60 °C for 1.5 h. The organic layer was separated and the aqueous layer was extracted with EtOAc. The organic layers were concentrated and purified by flash column chromatography over silica gel (20%-35% EtOAc/hexanes eluent) to give B-H09 (allyl 7-formyl-8-hydroxy-5-oxo-4,5-dihydro-1H-chromeno[3,4-c]pyridine-3(2H)-carboxylate) as a yellow solid (235 mg, 41%). <sup>1</sup>H NMR (400 MHz, CDCl<sub>3</sub>) δ 12.15 (s, 1H), 10.61 (s, 1H), 7.68 (d, *J* = 8.4 Hz, 1H), 6.92 (d, *J* = 9.0 Hz, 1H), 5.94 (m, 1H), 5.33 (m, 1H), 5.24 (m, 1H), 4.64 (d, *J* = 5.7 Hz, 2H), 4.47 (m, 2H), 3.81 (t, *J* = 5.8 Hz, 2H), 2.86 (m, 2H); <sup>13</sup>C NMR (101 MHz, CDCl<sub>3</sub>) δ 193.3, 164.9, 158.4, 155.2, 154.7, 146.4, 132.7, 131.8, 118.3, 117.2, 114.8, 111.2, 108.7, 66.7, 41.9, 39.2, 24.9; HRMS (ESI-TOF) (*m/z*) [M+H]<sup>+</sup> calcd for C<sub>17</sub>H<sub>16</sub>NO<sub>6</sub> 330.09721, found 330.09624.

*Synthesis of B-I08 (allyl 7-formyl-8-hydroxy-5-oxo-4,5-dihydro-1H-chromeno[3,4-c]pyridine-3(2H)-carboxylate)*

A solution of B-H09 in (150 mg, 455 μmol) in 4 mL of benzene was treated with 1,3-propanediol (99 μL, 1.4 mmol) and *p*-toluenesulfonic acid monohydrate (4.3 mg, 23 μmol) and stirred at reflux (85 °C) for 2 h. The reaction was quenched with 2 drops of triethylamine, diluted with EtOAc, and washed with brine. The organic layer was dried over Na<sub>2</sub>SO<sub>4</sub> and concentrated. Purification by flash column

chromatography over silica gel (30%-50% EtOAc/hexanes eluent) afforded B-I08 (allyl 7-formyl-8-hydroxy-5-oxo-4,5-dihydro-1H-chromeno[3,4-c]pyridine-3(2H)-carboxylate) as a yellow solid (157 mg, 89%). <sup>1</sup>H NMR (400 MHz, CDCl<sub>3</sub>) δ 8.82 (s, 1H), 7.36 (d, J = 8.2 Hz, 1H), 6.79 (d, J = 8.8 Hz, 1H), 6.28 (s, 1H), 5.91 (m, 1H), 5.30 (m, 1H), 5.20 (m, 1H), 4.61 (d, J = 5.6 Hz, 2H), 4.39 (s, 2H), 4.28 (dd, J = 11.6, J = 4.6 Hz, 2H), 4.09 (m, 2H), 3.74 (t, J = 5.8 Hz, 2H), 2.79 (m, 2H), 2.26 (m, 1H), 1.53 (m, 1H); <sup>13</sup>C NMR (101 MHz, CDCl<sub>3</sub>) δ 159.5, 159.3, 155.2, 150.5, 146.6, 132.8, 125.3, 118.0, 116.3, 114.5, 111.8, 109.9, 98.1, 67.9, 66.5, 41.8, 39.3, 25.8, 24.7; HRMS (ESI-TOF) (m/z) [M+H]<sup>+</sup> calcd for C<sub>20</sub>H<sub>22</sub>NO<sub>7</sub> 388.13908, found 388.13810.

#### *Synthesis of B-I09 (7-(1,3-dioxan-2-yl)-8-hydroxy-3,4-dihydro-1H-chromeno[3,4-c]pyridin-5(2H)-one)*

A solution of B-I08 (70 mg, 180 μmol) in 4 mL of DCM at rt was treated with phenylsilane (67 mg, 540 μmol) and tetrakis(triphenylphosphine)palladium(0) (10 mg, 9.0 μmol) and stirred at rt 25 min. The reaction was concentrated and the residue purified by flash chromatography over silica gel (0%-10% MeOH/CHCl<sub>3</sub> eluent) to afford B-I09 (7-(1,3-dioxan-2-yl)-8-hydroxy-3,4-dihydro-1H-chromeno[3,4-c]pyridin-5(2H)-one) as a yellow solid (54 mg, 98%). <sup>1</sup>H NMR (400 MHz, CDCl<sub>3</sub>) δ 7.35 (d, J = 8.8 Hz, 1H), 6.78 (d, J = 8.8 Hz, 1H), 6.28 (s, 1H), 4.24 (m, 2H), 4.06 (m, 2H), 3.75 (m, 2H), 3.11 (t, J = 5.8 Hz, 2H), 2.70 (m, 2H), 2.36 – 2.11 (m, 1H), 1.92 (bs, 1H), 1.50 (m, 1H); <sup>13</sup>C NMR (101 MHz, CDCl<sub>3</sub>) δ 160.2, 159.0, 150.6, 146.8, 135.0, 125.1, 119.0, 114.3, 112.5, 109.9, 98.3, 68.0, 43.4, 42.0, 25.9, 25.3; HRMS (ESI-TOF) (m/z) [M+H]<sup>+</sup> calcd for C<sub>16</sub>H<sub>18</sub>NO<sub>5</sub> 304.11795, found 304.11782.

#### *Synthesis of biotinylated derivatives B-I06 and B-I07*

A solution of B-I09 (46 mg, 150 μmol) in 3 mL of DCM:MeCN (1:1) was treated with triethylamine (43 μL, 300 μmol) and biotinamidohexanoyl-6-aminohexanoic acid N-hydroxysuccinimide ester (76 mg, 170 μmol) and the reaction was stirred at rt for 20 h. The mixture was concentrated under reduced pressure and purified by flash column chromatography over silica gel (30%-50%

EtOAc/hexanes eluent) to give *N*-(6-(7-(1,3-dioxan-2-yl)-8-hydroxy-5-oxo-1*H*-chromeno[3,4-*c*]pyridin-3(2*H*,4*H*,5*H*)-yl)-6-oxohexyl)-5-((3*aS*,4*S*,6*aR*)-2-oxohexahydro-1*H*-thieno[3,4-*d*]imidazol-4-yl)pentanamide as a yellow solid (96 mg, 96%). <sup>1</sup>H NMR (400 MHz, CDCl<sub>3</sub>) δ 8.83 (m, 1H), 7.35 (m, 1H), 6.79 (m, 1H), 6.74-6.40 (m, 2H), 6.26 (s, 1H), 5.81(bs, 1H), 4.44 (m, 2H), 4.33 (bs, 1H), 4.23 (m, 3H), 4.06 (m, 2H), 3.80 (m, 1.5H), 3.68 (m, 0.5H), 3.17 (m, 2H), 3.06 (m, 1H), 2.84 (m, 1H), 2.76 (m, 1H), 2.66 (m, 1H), 2.54 (m, 1H), 2.37 (m, 2H), 2.24 (m, 1H), 2.11 (m, 2H), 1.73 – 1.42 (m, 9H), 1.41 – 1.22 (m, 4H); <sup>13</sup>C NMR (101 MHz, CDCl<sub>3</sub>) δ 173.7, 173.5, 173.5, 172.2, 171.9, 169.6, 168.7, 164.3, 164.3, 159.7, 159.6, 159.4, 159.3, 150.6, 147.7, 145.8, 125.5, 125.3, 116.8, 115.7, 114.8, 114.5, 111.7, 111.6, 109.9, 98.1, 68.0, 61.9, 61.8, 60.3, 55.9, 43.2, 41.4, 40.7, 40.2, 39.2, 39.1, 39.1, 37.3, 36.1, 36.0, 33.6, 33.1, 30.9, 29.2, 28.9, 28.3, 28.3, 28.1, 26.6, 25.9, 25.9, 25.8, 25.7, 24.7, 24.6, 24.3; HRMS (ESI-TOF) (*m/z*) [M+H]<sup>+</sup> calcd for C<sub>32</sub>H<sub>43</sub>N<sub>4</sub>O<sub>8</sub>S 643.27961, found 643.27695.

A solution of the above intermediate (40 mg, 72 μmol) in 1.5 mL of acetone was treated with 4N aq. HCl and stirred for 4 h at rt. The reaction was concentrated and the crude product was purified by semipreparative RP-HPLC (C<sub>18</sub> 9.4 x 250 mm column, 20–100% MeCN/H<sub>2</sub>O linear gradient, 20 min) to afford B-106 as a white solid (19 mg, 52%). <sup>1</sup>H NMR (400 MHz, CDCl<sub>3</sub>) δ 12.16 (m, 1H), 10.61 (m, 1H), 7.69 (m, 1H), 6.93 (m, 1H), 6.51 (m, 0.5H), 6.33 (m, 1.5H), 5.58 (m, 1H), 4.52 (m, 2H), 4.44 (s, 1H), 4.32 (m, 1H), 3.91 (t, *J* = 5.6 Hz, 1H), 3.79 (t, *J* = 5.4 Hz, 1H), 3.25 (m, 2H), 3.13 (m, 1H), 2.89 (m, 3H), 2.72 (m, 1H), 2.45 (t, *J* = 7.1 Hz, 2H), 2.20 (t, *J* = 7.2 Hz, 2H), 1.91 (bs, 1H), 1.69 (m, 6H), 1.53 (m, 1.5H), 1.41 (m, 3.5H); <sup>13</sup>C NMR (101 MHz, CDCl<sub>3</sub>) δ 193.2, 173.4, 172.3, 165.1, 164.0, 158.7, 154.7, 147.6, 132.0, 116.9, 115.0, 114.8, 111.2, 108.7, 61.9, 60.3, 55.8, 43.2, 40.7, 39.2, 37.2, 36.1, 33.6, 29.3, 28.3, 28.1, 26.6, 25.8, 24.9, 24.5; HRMS (ESI-TOF) (*m/z*) [M+H]<sup>+</sup> calcd for C<sub>29</sub>H<sub>37</sub>N<sub>4</sub>O<sub>7</sub>S 585.23775, found 585.23708.

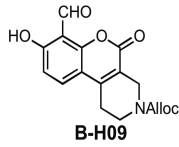
Negative control compound B-107 was obtained by dissolving B-106 (25 mg, 42 μmol) in 2 mL of MeOH and adding sodium borohydride (1.6 mg, 42 μmol). After stirring 3 h, the reaction was quenched with 1M aq. HCl and extracted with chloroform. The organic layer was concentrated and the crude

product was purified by semipreparative RP-HPLC ( $C_{18}$  9.4 x 250 mm column, 40–90% MeCN/H<sub>2</sub>O linear gradient, 20 min) to afford B-I07 as a white solid (7 mg, 28%); <sup>1</sup>H NMR (400 MHz, DMOS-d<sub>6</sub>)  $\delta$  8.44 (bs, 1H), 7.75 (m, 1H), 7.34 (m, 1H), 6.56 (d,  $J$  = 8.6 Hz, 1H), 6.42 (m, 1H), 6.35 (m, 1H), 4.75 (s, 2H), 4.27 (d,  $J$  = 6.2 Hz, 3H), 4.08 (m, 1H), 3.69 (m, 2H), 3.08 (m, 0.3H), 2.99 (m, 1.7H), 2.89 (m, 1H), 2.77 (m, 2H), 2.56 (m, 1H), 2.36 (m, 2H), 2.01 (t,  $J$  = 7.3 Hz, 2H), 1.67 – 1.11 (m, 14H); <sup>13</sup>C NMR (101 MHz, DMSO)  $\delta$  172.2, 171.5, 163.1, 149.3, 122.8, 114.9, 113.9, 113.6, 112.6, 109.4, 109.3, 105.0, 61.5, 59.6, 56.6, 55.9, 38.7, 35.7, 32.8, 29.5, 28.7, 28.5, 26.6, 25.8, 24.9, 24.7; HRMS (ESI-TOF) ( $m/z$ ) [M+H]<sup>+</sup> calcd for C<sub>29</sub>H<sub>39</sub>N<sub>4</sub>O<sub>7</sub>S 587.25395, found 587.25300.

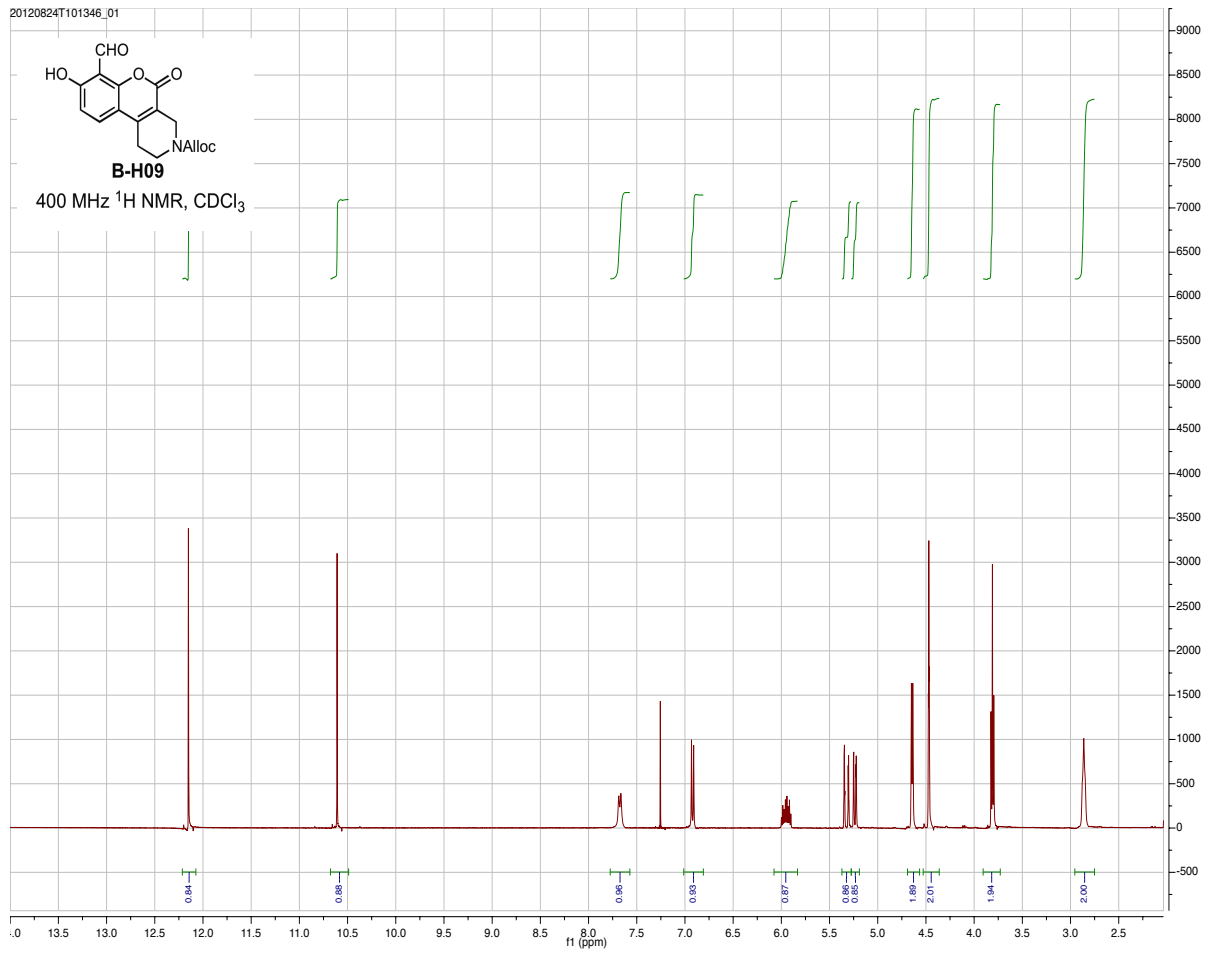
#### *B-I09 degradation studies*

A 20 mM stock solution of B-I09 in DMSO was diluted to 0.5 mM in FRET assay buffer (20 mM HEPES, pH 7.5, 50 mM KOAc, 0.5 mM MgCl<sub>2</sub>, 3 mM DTT, 0.4% PEG) or cell culture media (RPMI supplemented with 10% fetal bovine serum). The FRET assay buffer and cell culture media solutions were incubated at room temperature and 37 °C, respectively. At various timepoints, a 50  $\mu$ L aliquot of each solution was added to 50  $\mu$ L of methanol and the mixture analyzed by analytical reverse-phase HPLC ( $C_{18}$  4mm x 150mm column, 1 mL/min flow rate) with acetonitrile/water (0.1% formic acid) as eluent. Absorbance was read at 320 nm and the degradation product (aldehyde; C-B06) was identified by LCMS and co-injection with pure synthetic sample. Degradation studies were carried out in duplicate and data points reported as the mean of two values.

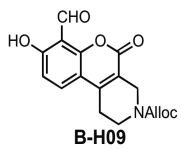
20120824T101346\_01



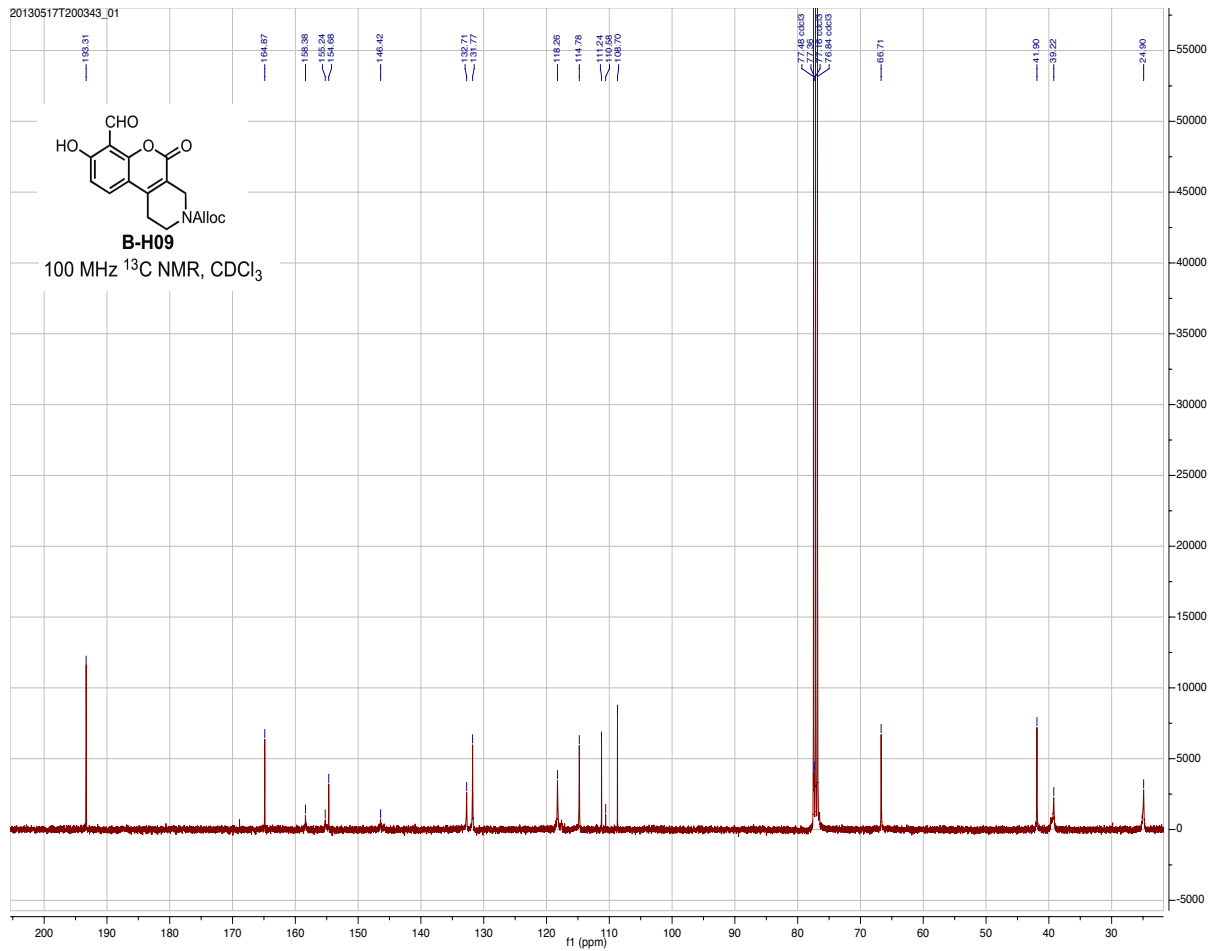
400 MHz <sup>1</sup>H NMR, CDCl<sub>3</sub>



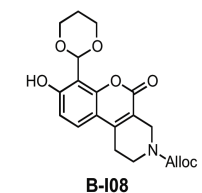
20130517T200343\_01



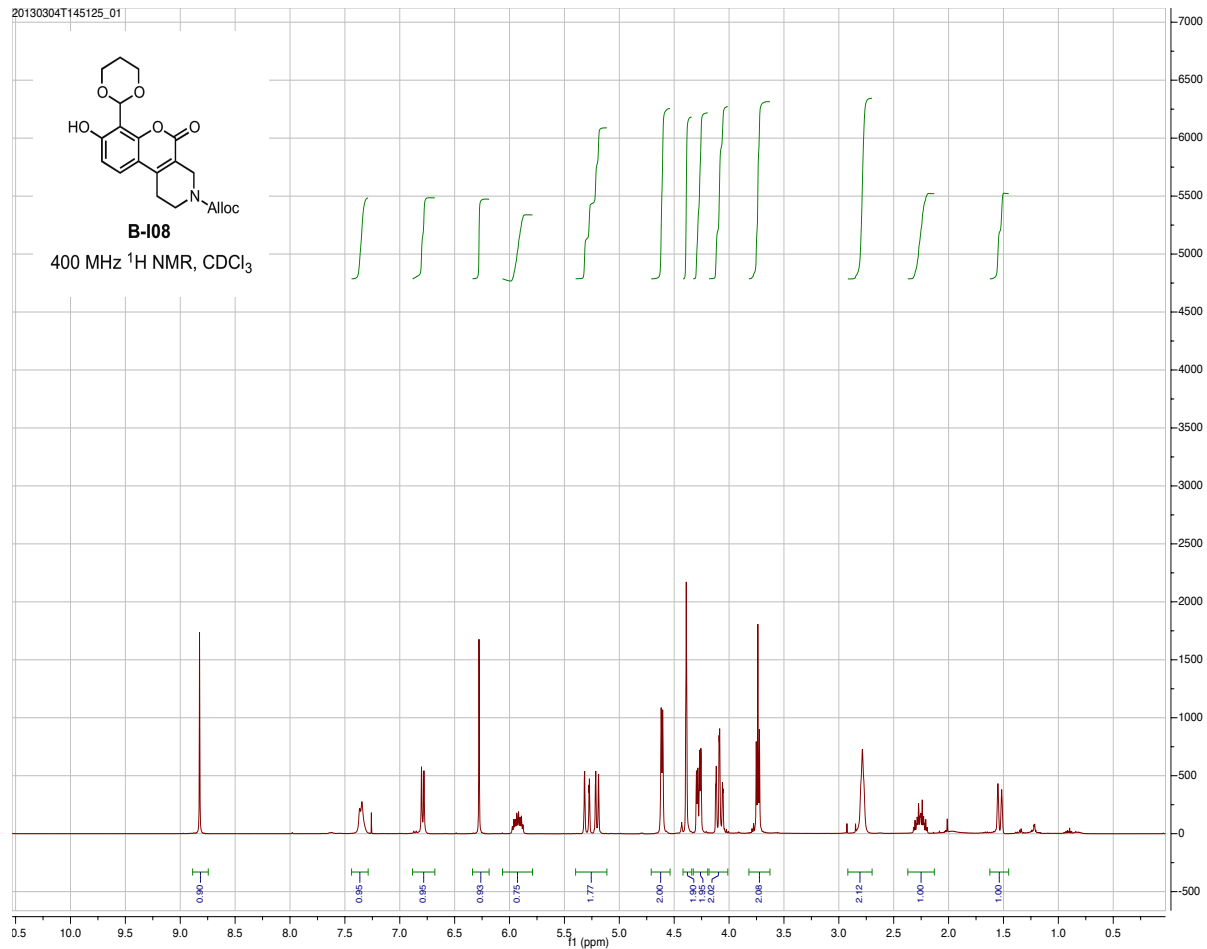
100 MHz <sup>13</sup>C NMR, CDCl<sub>3</sub>



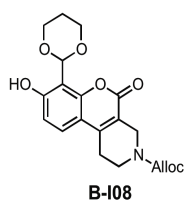
20130304T145125\_01



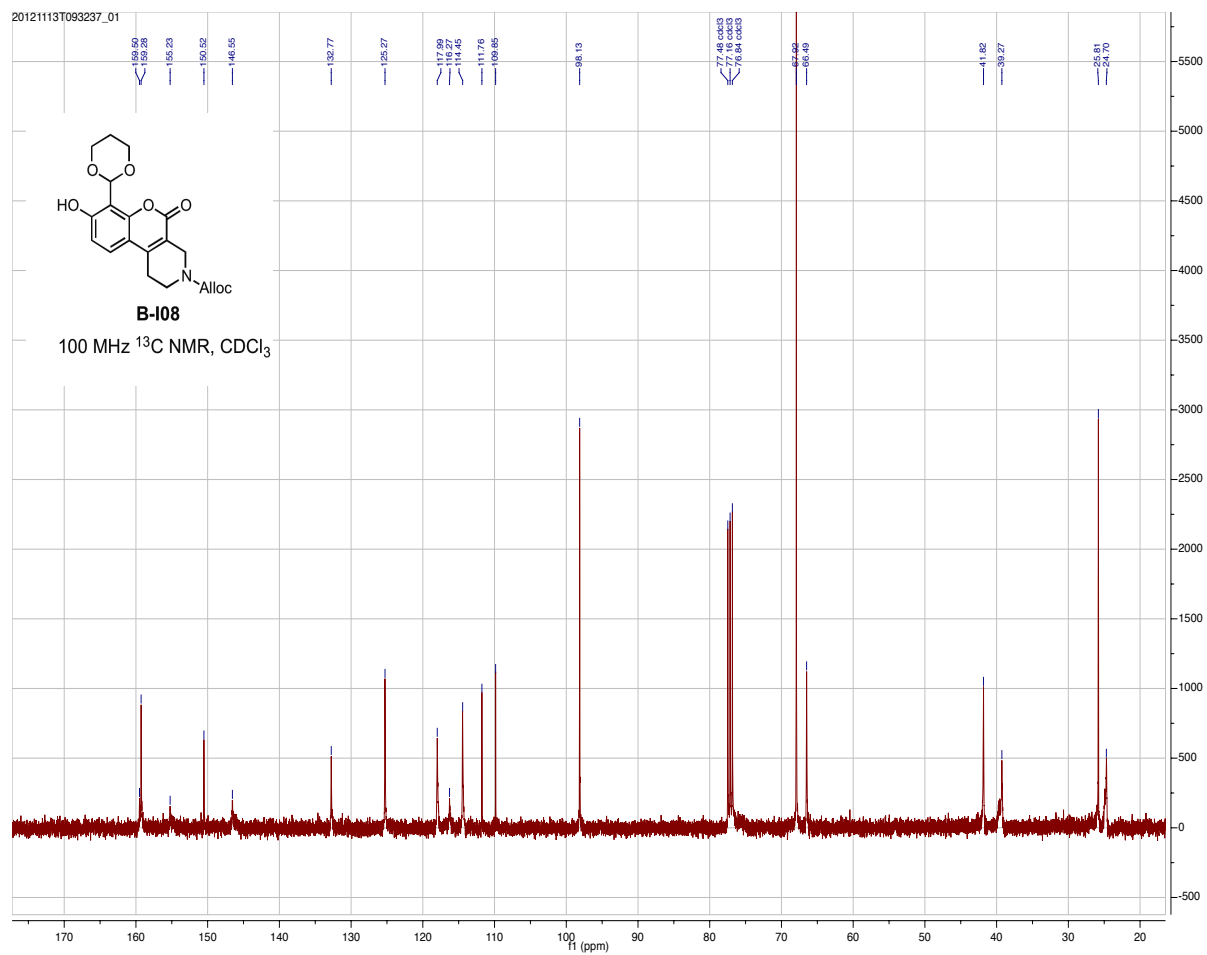
400 MHz <sup>1</sup>H NMR, CDCl<sub>3</sub>



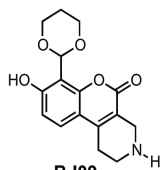
20121113T093237\_01



100 MHz <sup>13</sup>C NMR, CDCl<sub>3</sub>

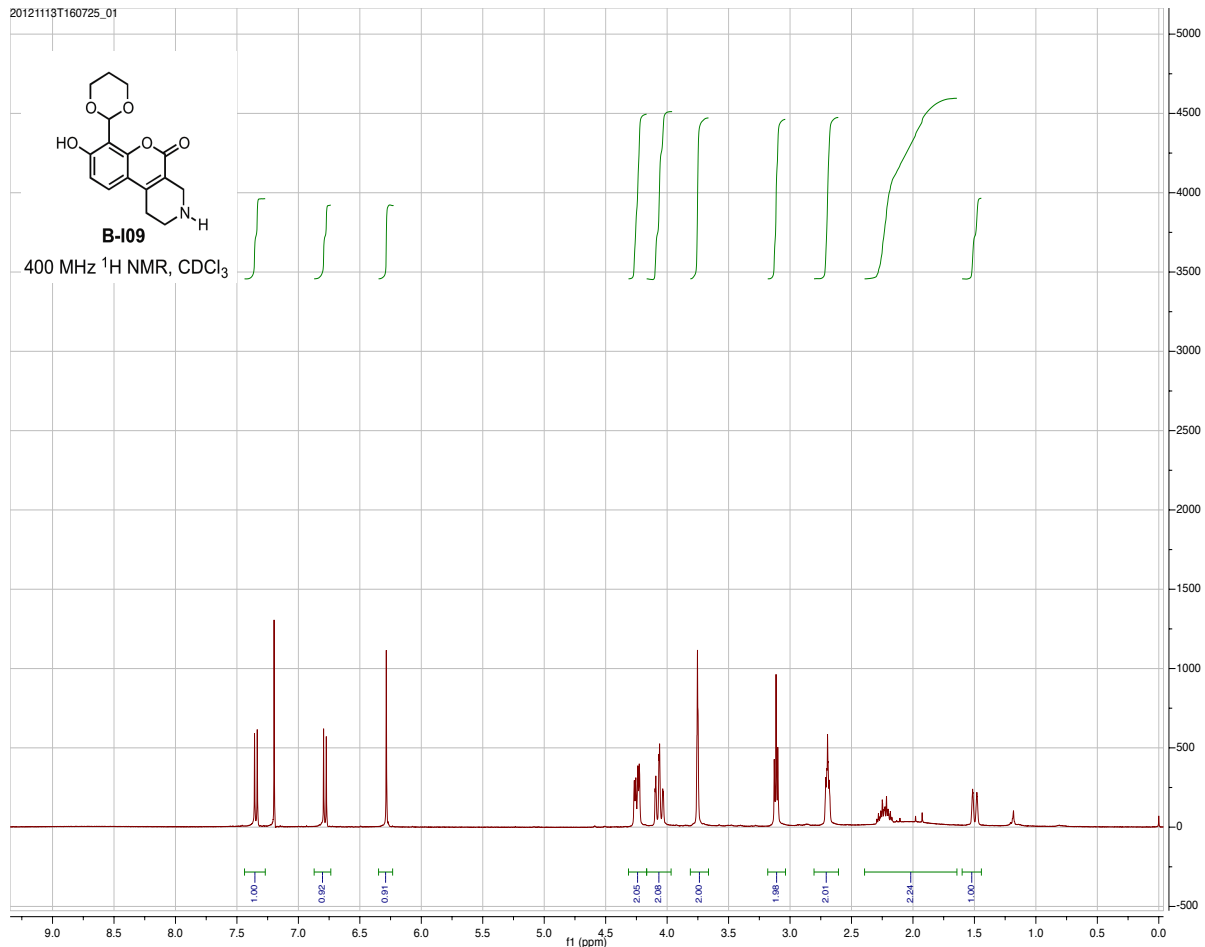


20121113T160725\_01

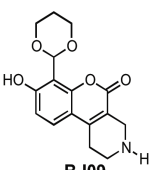


**B-109**

400 MHz  $^1\text{H}$  NMR,  $\text{CDCl}_3$

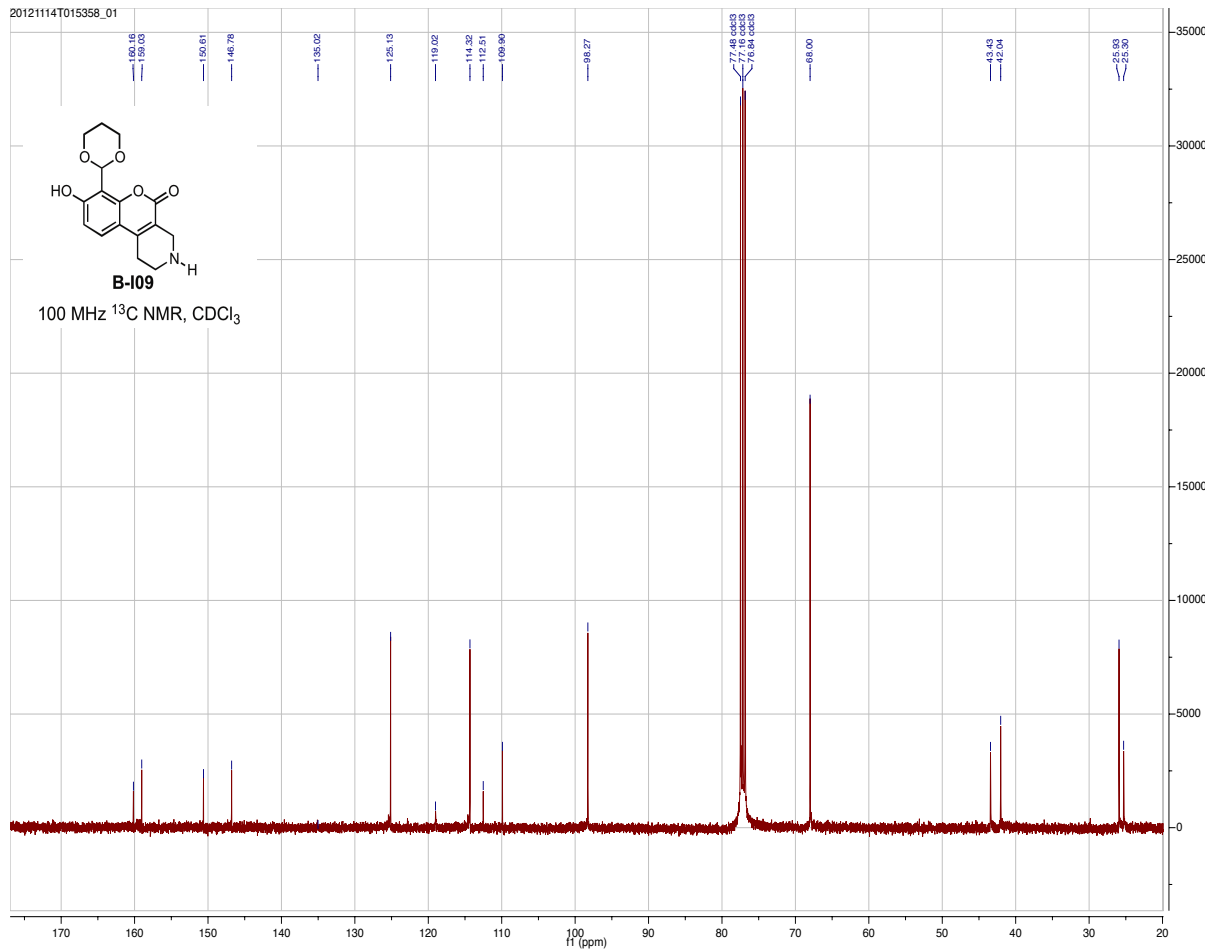


20121114T015358\_01

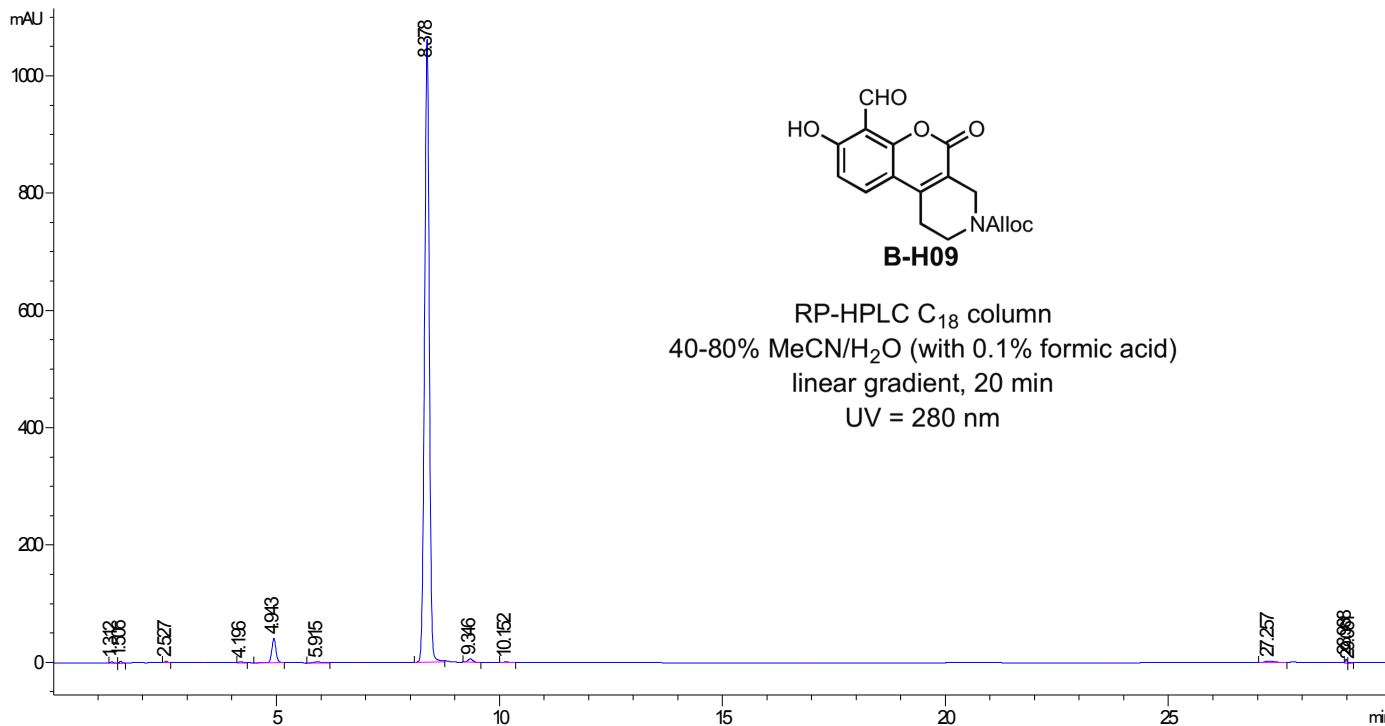


**B-109**

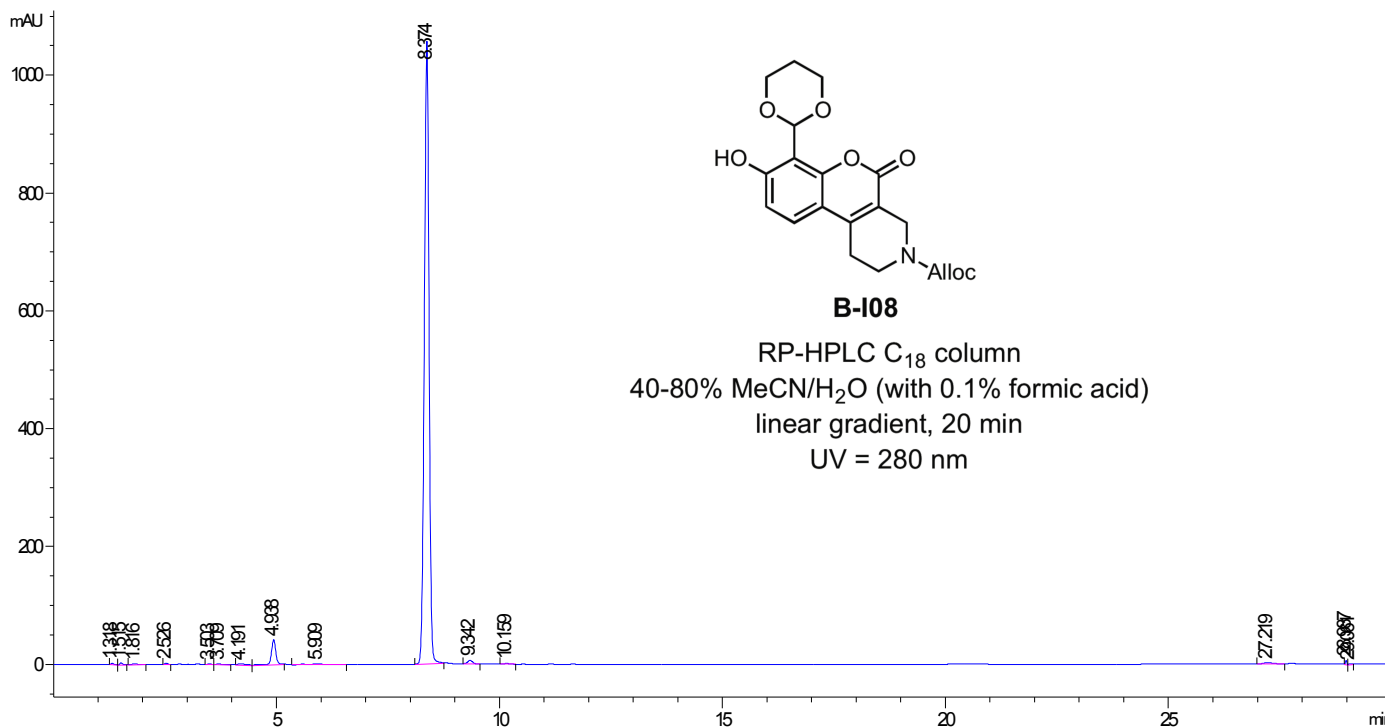
100 MHz  $^{13}\text{C}$  NMR,  $\text{CDCl}_3$

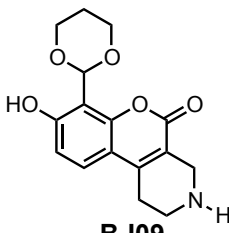
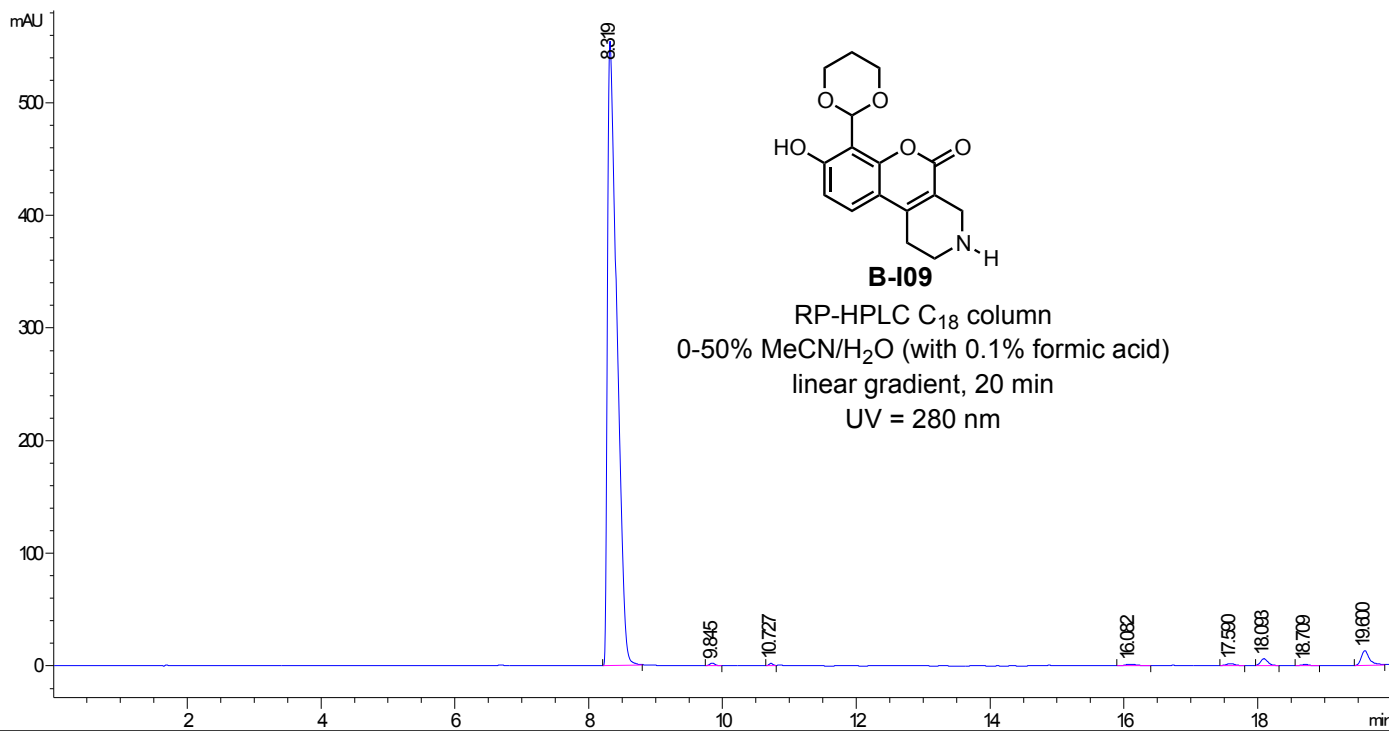


DAD1 E, Sg=280,16 Ref=360,100 (JRD,JRD 2013-04-17 13:02:58,001-0101.D)



DAD1 E, Sg=280,16 Ref=360,100 (JRD,JRD 2013-04-17 13:02:58,001-0201.D)





**B-109**

RP-HPLC C<sub>18</sub> column  
0-50% MeCN/H<sub>2</sub>O (with 0.1% formic acid)  
linear gradient, 20 min  
UV = 280 nm

Fig. S1

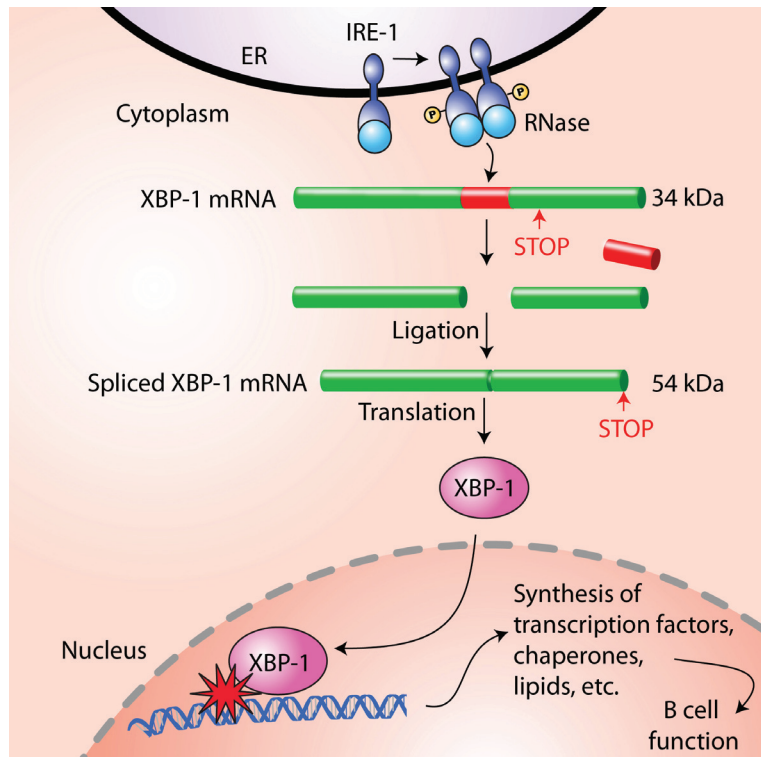
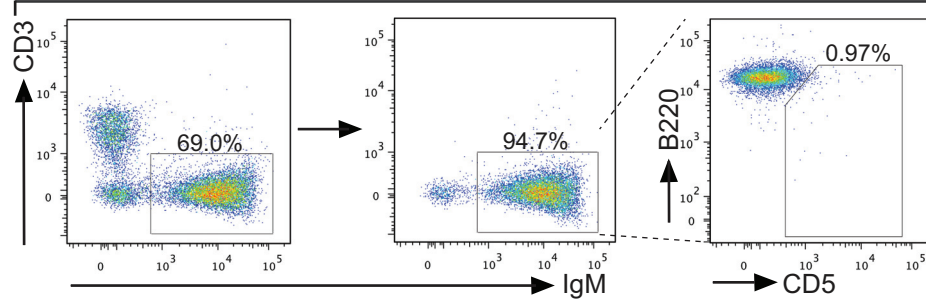
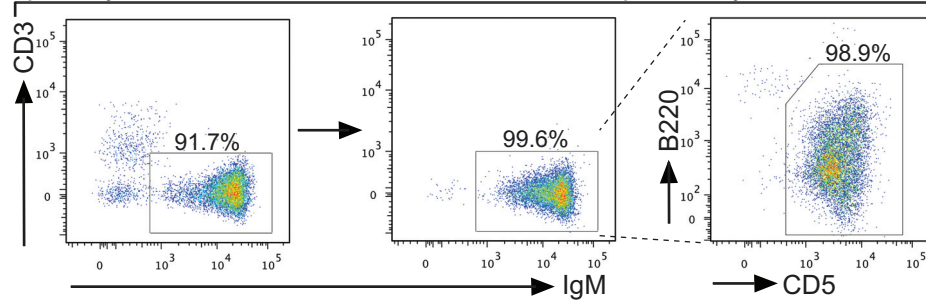


Fig. S2

A Splenocytes from 6-week-old XBP-1<sup>WT</sup>/TCL1 mice purified by Pan-B MicroBeads



B Splenocytes from 14-month-old XBP-1<sup>WT</sup>/TCL1 mice purified by Pan-B MicroBeads



C Splenocytes from 14-month-old XBP-1<sup>KO</sup>/TCL1 mice purified by Pan-B MicroBeads

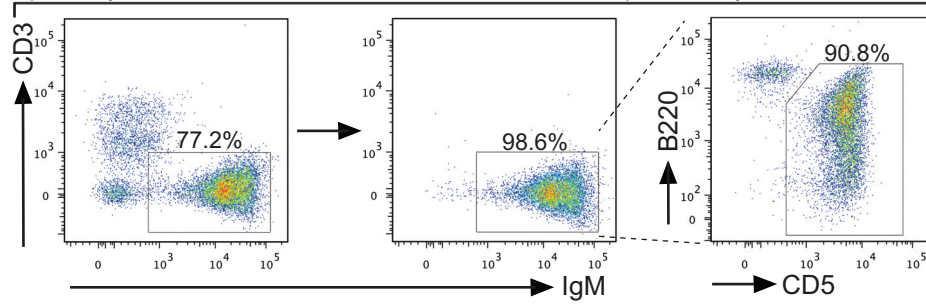


Fig. S3

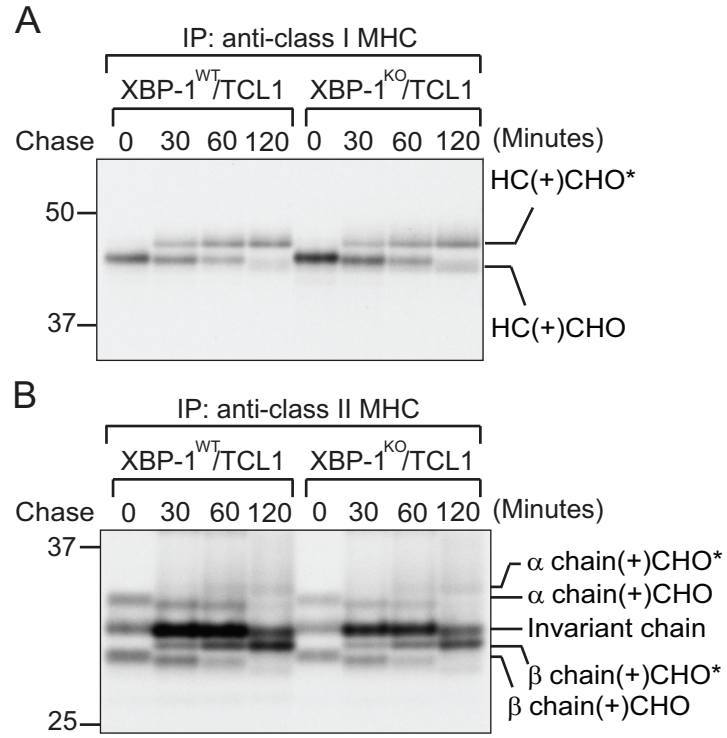


Fig. S4

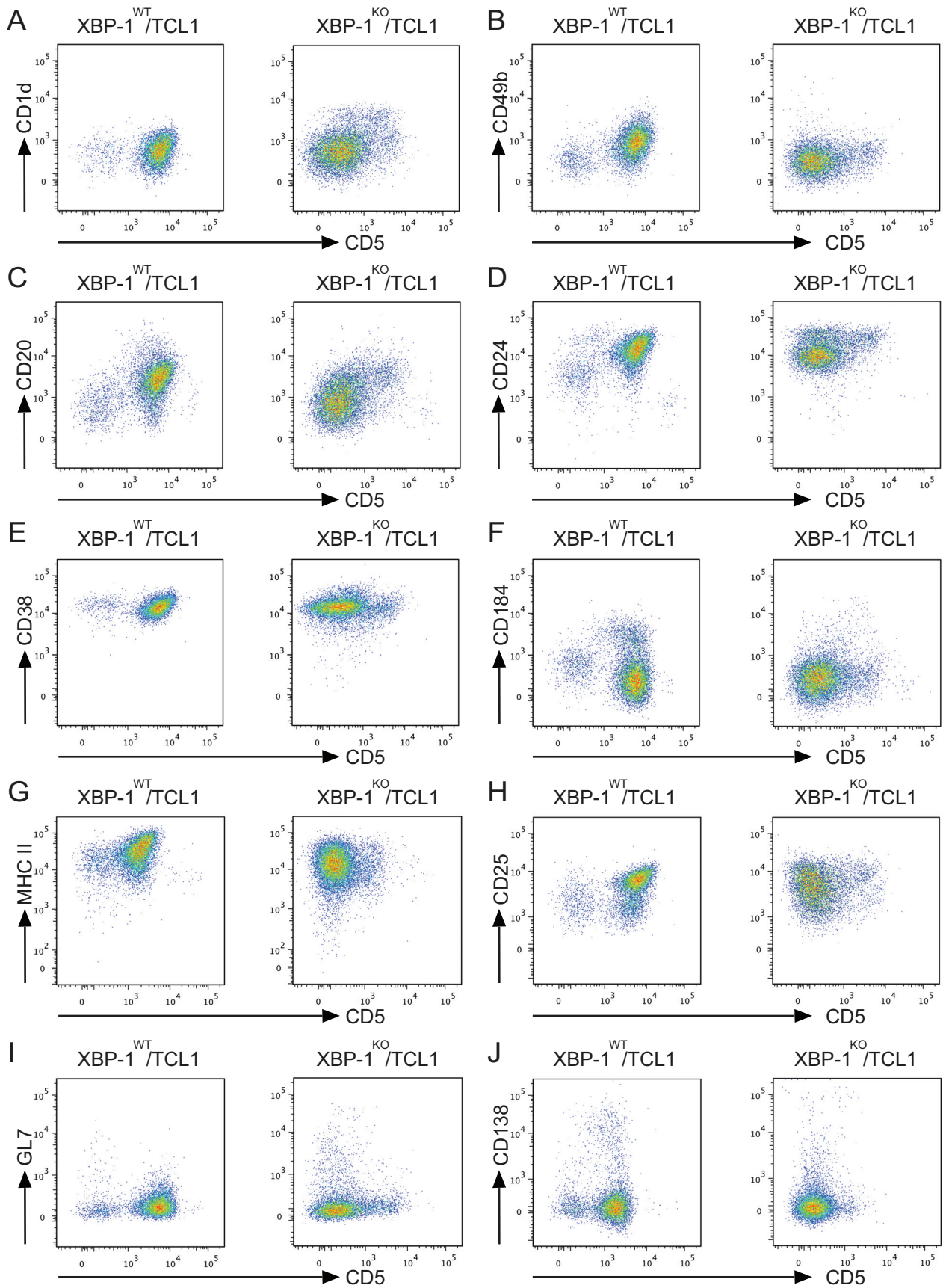


Fig. S5

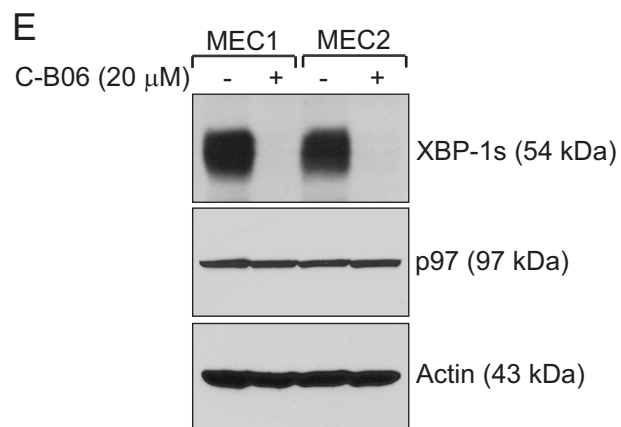
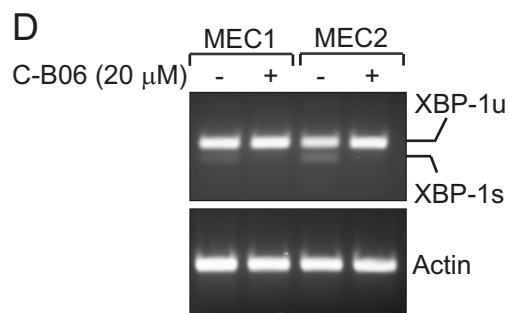
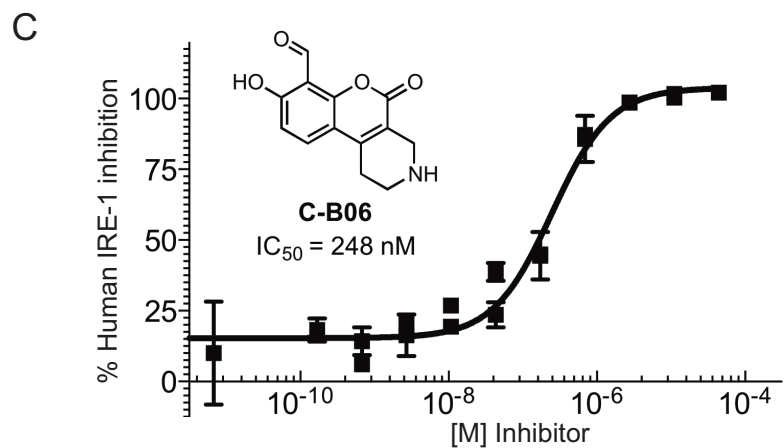
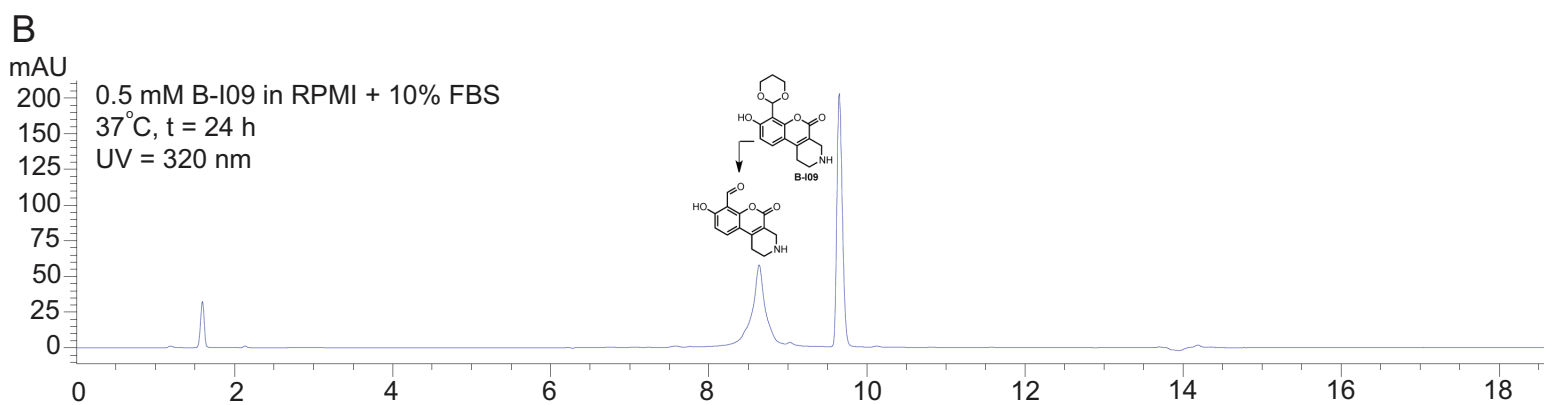
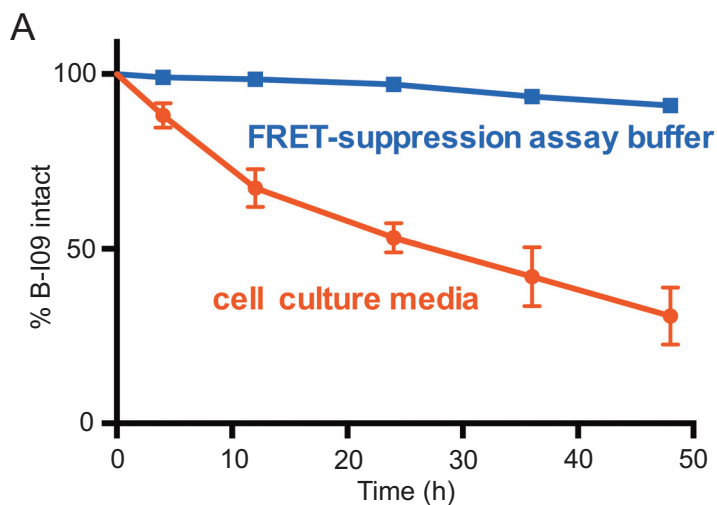


Fig. S6

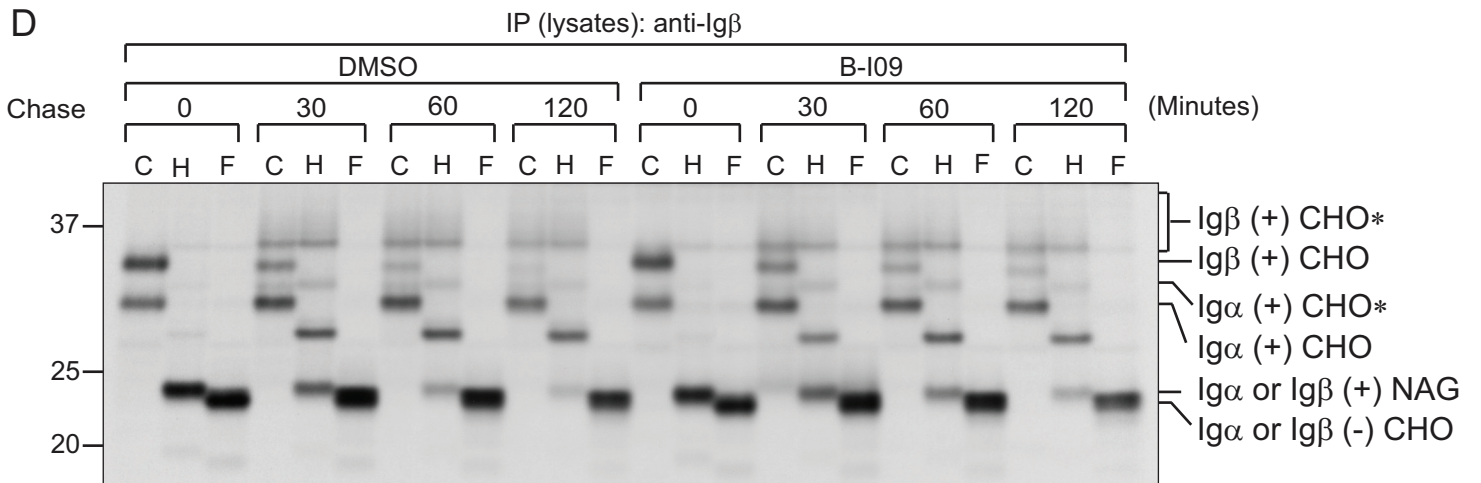
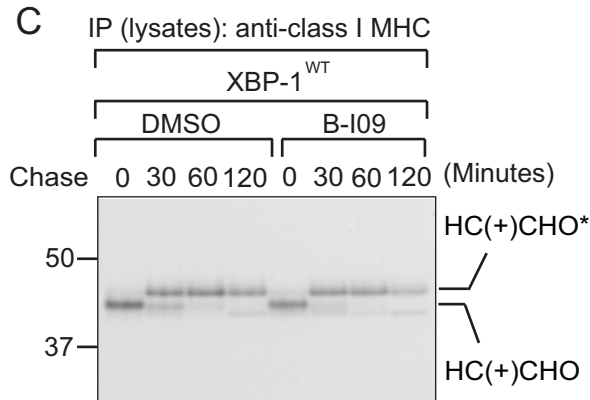
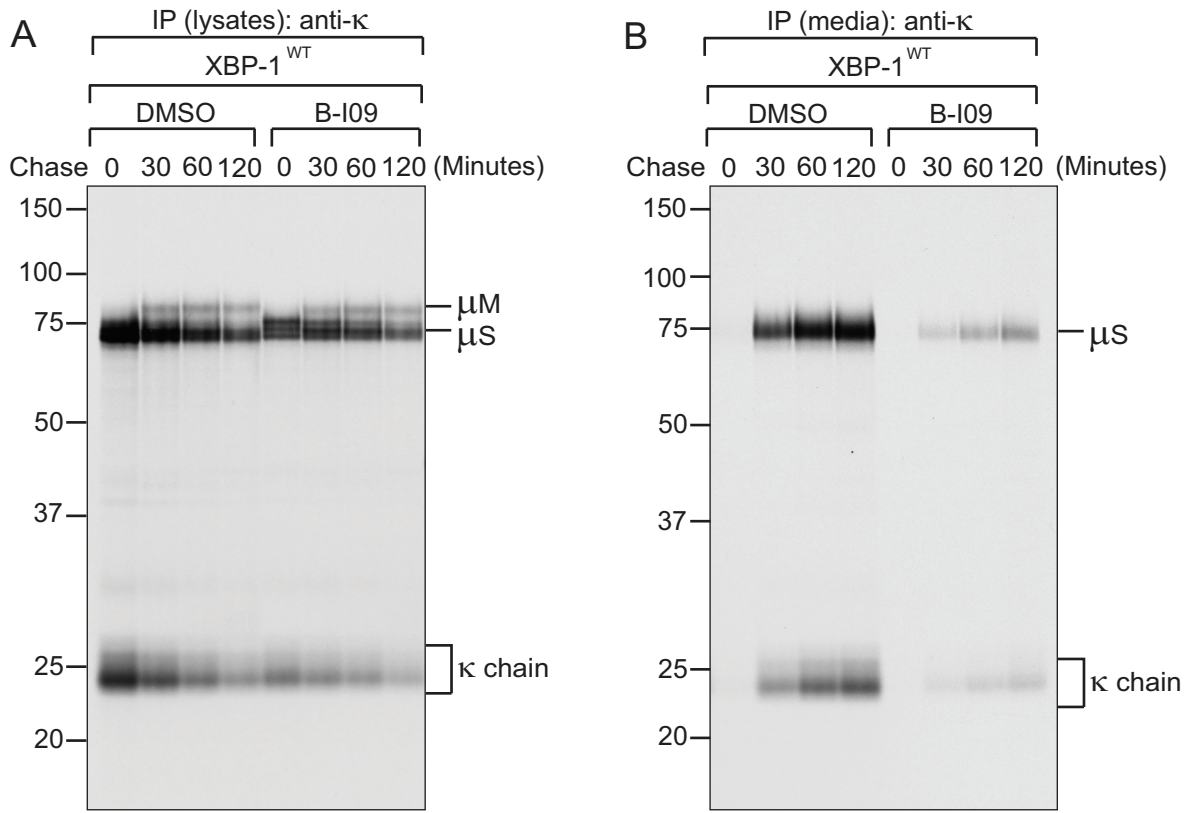


Fig. S7

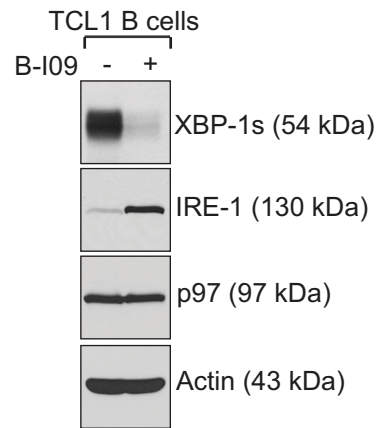


Fig. S8

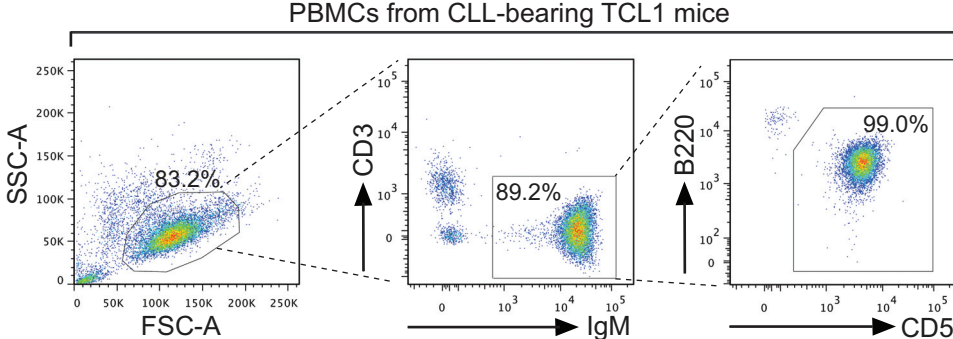
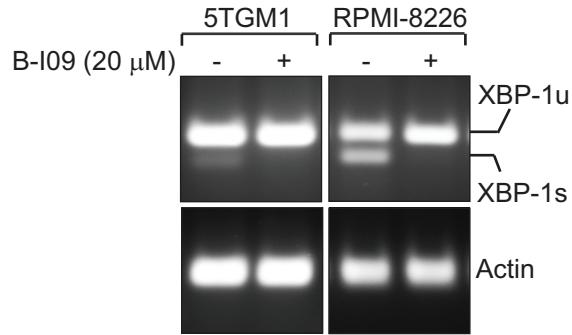
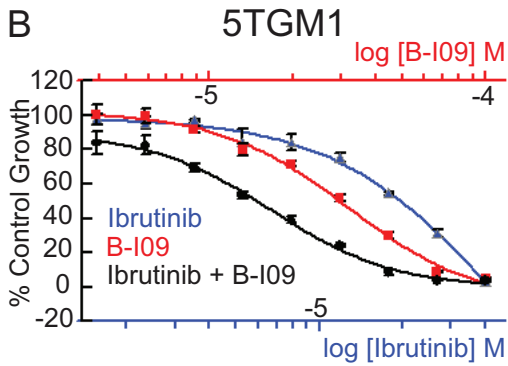


Fig. S9

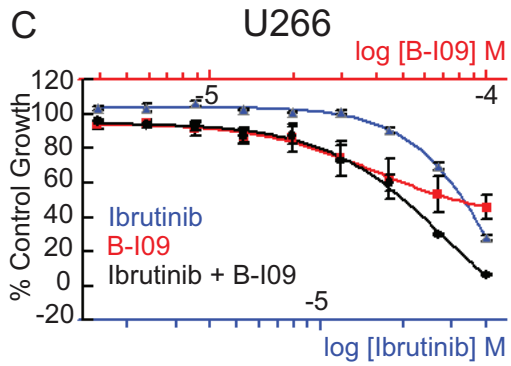
A



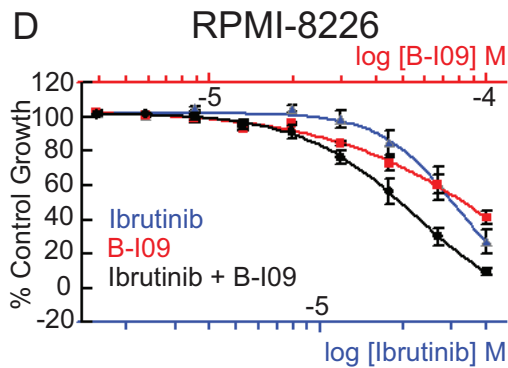
B



C



D



E

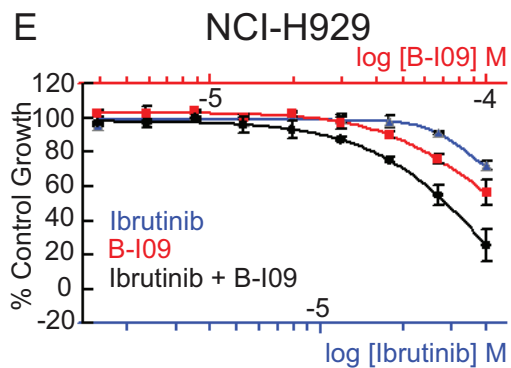


Fig. S10

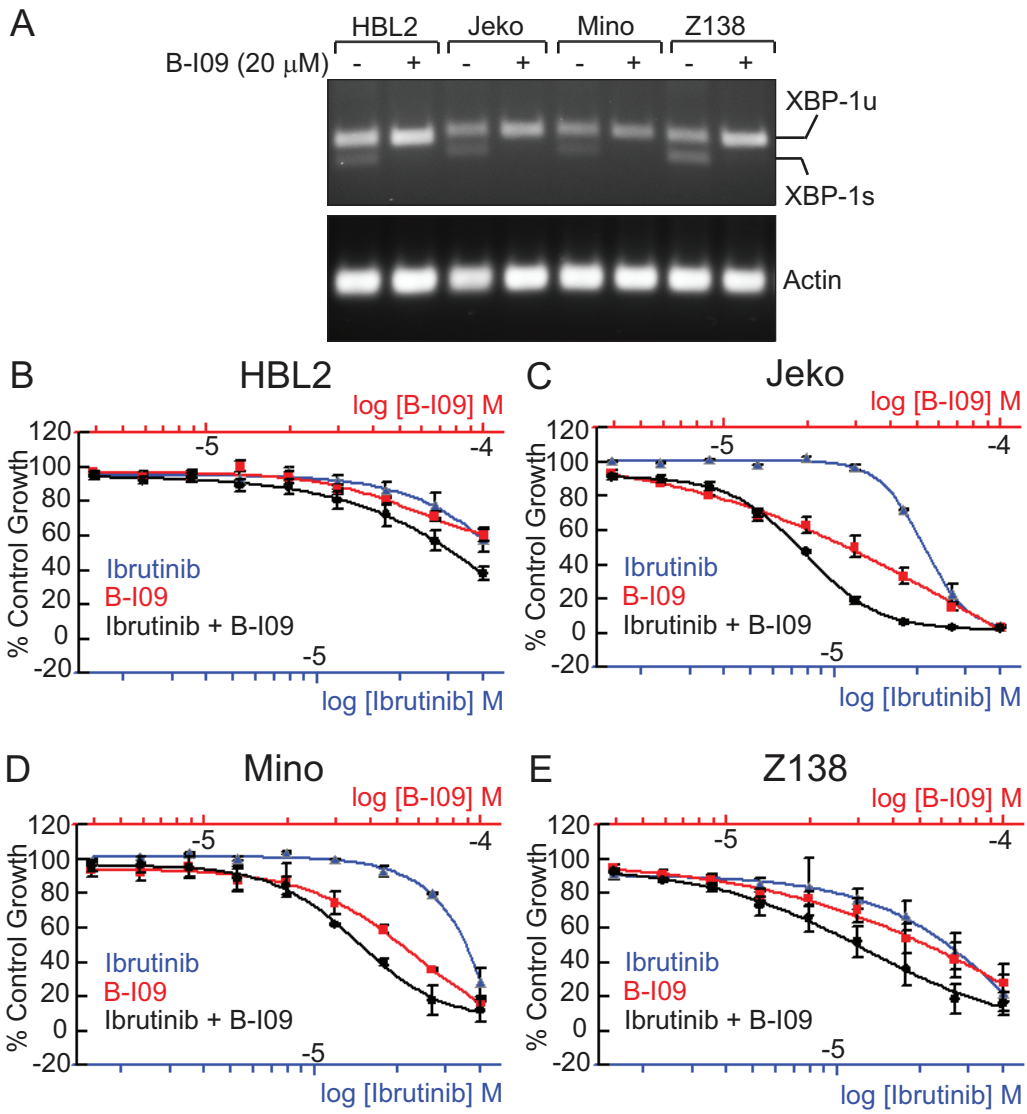


Fig. S11

